Earthquakes and Structures, *Vol. 18, No. 2 (2020) 233-248*
DOI: https://doi.org/10.12989/eas.2020.18.2.233

Comparison of different distributions of viscous damper properties in asymmetric-plan frames

Luca Landi*, Andrea Molari and Pier Paolo Diotallevi

Department DICAM, University of Bologna, Viale Risorgimento 2, Bologna 40136, Italy

(*Received August 5, 2018, Revised October 25, 2019, Accepted January 4, 2020*)

Abstract. In this article, one of the procedures to design viscous dampers proposed in literature is applied to 3D asymmetric-plan buildings, considering different distributions for the damping coefficients, which are assumed to be proportional to specific structural or response parameters. The main purpose was to investigate the effectiveness of different vertical and in-plan distributions of the damping coefficients of nonlinear viscous dampers for the seismic retrofit of existing buildings. For comparison purposes, all the distributions were applied utilizing both a simplified and an extended method for the 3D structures, where the simplified method takes into account only the translation in the seismic direction, and the extended method considers the translations along the two orthogonal directions together with the floor rotations. The proposed distributions were then applied to a typical case study involving an asymmetric-plan six-storey RC building. The effectiveness of the different distributions was examined through time-history analyses, assuming nonlinear behaviour for both the viscous dampers and the structural elements. The results of the nonlinear dynamic analyses were examined in terms of maximum and residual inter-storey drifts, peak floor accelerations and maximum damper forces.

Keywords: damping distribution; seismic retrofit; asymmetric-plan structures; existing buildings; nonlinear viscous dampers; design procedure; nonlinear dynamic analysis

1. Introduction

The issue of the rehabilitation of existing buildings has been debated extensively over the past years because of the large number of inadequate existing structures in seismic zones. Public and strategic buildings in particular have to withstand stronger earthquakes than ordinary buildings. For these buildings, the retrofit objective of satisfying the seismic requirements of new buildings often becomes economically prohibitive. In these cases, dissipating seismic energy by added damping devices can be a very promising solution for improving seismic performance, since less energy is dissipated through the structural elements and less damage occurs (Constantinou *et al.* 1998, Chopra 2001, Christopoulos and Filiatrault 2006). Fluid-viscous dampers provide several benefits (Symans and Constantinou 1998, Miyamoto *et al*. 2002,), since the damping coefficient is independent of frequency and their energy dissipation capacity is very high. The behaviour of viscous dampers can be linear or nonlinear as a function of the exponent of the velocity, which in the latter case is defined by values lower than one. The advantage of nonlinear viscous dampers is that the force in the damper can be controlled to avoid overloading the damper or the system to which it is connected when there is a large increase in velocity. Various studies have investigated the design criteria for inserting and distributing the dampers in building structures (Dargush and Sant 2005, Sorace and Terenzi 2008, Mazza and Vulcano 2011, Silvestri *et al.* 2011, Sullivan and Lago 2012, Hwang *et al*. 2013, Palermo *et al*. 2013, Whittle *et al*. 2013, Landi *et al*. 2014), with a great many being concerned with the development of methodologies and algorithms to search for the optimal damper configuration (Hahn and Sathiavageeswaran 1992, Takewaki 1997, Takewaki *et al*. 1999, Lopez Garcia 2001, Singh and Moreschi 2001, Lopez Garcia and Soong 2002, Garcia *et al*. 2007, Lavan and Levi 2010, Aguirre *et al*. 2012, Fujita *et al.* 2014, Altieri *et al.* 2018, Huang 2018). The optimal damper distribution in plan and along the height can be found through optimization techniques, though they are computationally expensive (Tubaldi *et al.* 2015, Pollini *et al.* 2017).

More simplified approaches have been also proposed in literature on the basis of simple design formulae. The simplified procedures for designing nonlinear viscous dampers are often based on the assessment of the added and the effective damping ratio (Ramirez *et al*. 2000, Ramirez *et al*. 2002, Diotallevi *et al*. 2012). One of these, in particular, which was originally proposed for symmetric structures, involves evaluating the damping ratio of Multi-Degree-of-Freedom (MDOF) systems and accounts for the nonlinear behaviour of the structure (Ramirez *et al*. 2000). Some of the authors of the present research subsequently extended this procedure to asymmetric-plan structures, considering damping coefficients with a vertical and in-plan uniform distribution (Landi *et al*. 2013). In another study by some authors of the present research, various vertical distributions of the damping coefficients were examined in regular and

*Corresponding author, Associate Professor
E-mail: l.landi@unibo.it

http://www.techno-press.org/?journal=eas&subpage=7 ISSN: 2092-7614 (Print), 2092-7622 (Online)

irregular plane frames (Landi *et al.* 2015), and the distribution of the coefficients was defined as a function of the different structural properties. The main purpose of the research presented here is to extend the studies mentioned above by investigating whether the different distributions of damping coefficients can be applied to general asymmetric-plan RC structures. In detail, the aim is to extend the previous design procedure by varying both the vertical and in-plan distributions of the damping coefficients for buildings with varying structural properties along the height and the plan in order to improve the design of the damping system. Two different methods are examined when designing the damping system, where the former is based only on the translations of the structure in the seismic direction (simplified method), and the latter on the translations along two orthogonal directions and on the floor rotations (extended method). The proposed distributions and methods are then applied to a typical case study of an asymmetric-plan six-storey RC building.

The effectiveness of the different distributions is evaluated by performing several nonlinear dynamic analyses (NLDA), assuming nonlinear behaviour for both the structural elements and the fluid-viscous dampers. The response parameters involved are the maximum inter-story drifts, the residual inter-story drifts and the peak floor accelerations. In addition, important information about the costs of the distributions are derived by examining the damping coefficients, obtained from the design procedure, as well as the maximum damper forces, evaluated through NLDA.

2. Framing of the procedure: determination of seismic demand with supplemental damping

Seismic demand is determined according to a procedure based on the comparison between the capacity and demand spectra in the acceleration-displacement graphical representation (Ramirez *et al.* 2000). The first is derived through a nonlinear static analysis, and the latter is obtained by reducing the elastic response spectrum corresponding to the considered limit state as a function of the effective global damping ratio of the building. The intersection between the capacity curve and the demand spectrum gives the performance point and the actual displacement demand.

To apply the procedure, a bilinear idealization of the capacity spectrum is needed in order to obtain the elastic stiffness, yielding point and post-elastic stiffness of the equivalent Single-Degree-of-Freedom (SDOF) structure. An effective period equivalent to the actual structure is then associated to the SDOF system (Priestley *et al.* 2007). This period is calculated using the secant stiffness at the maximum displacement, which corresponds to the displacement demand.

The effective global damping ratio ξ_{eff}, used to determine the damping reduction factor of the spectral ordinates (FEMA 450 2003, Lin and Chang 2003), can be derived as the sum of three terms (Ramirez 2000): the inherent damping ratio ξ_i, the hysteretic damping ratio ξ_h and the supplemental damping ratio provided by the dampers ξ_v

$$\xi_{eff} = \xi_i + \xi_h + \xi_v \tag{1}$$

The hysteretic contribution is related to the nonlinear behaviour of the structural members and is present only if the structure exceeds the elastic limit. In addition, the contribution provided by the dampers, in the presence of nonlinear structural response, includes the effect of ductility. If the bilinear idealization of the capacity curve has a negligible post-elastic stiffness, or is an elastic-perfectly plastic diagram, Eq. (1) can be redrafted as follows

$$\xi_{eff} = \xi_i + \frac{2q_h}{\pi}\left(1 - \frac{1}{\mu_D}\right) + \xi_{ve}(\mu_D)^{1-\frac{\alpha}{2}} \tag{2}$$

where q_h is a factor equal to the ratio of the actual area of hysteresis loop to that of the assumed perfect bilinear oscillator and μ_D is the ductility demand. This factor is, therefore, related to the quality of the structural system in terms of its dissipative capacity. Several indications for defining q_h can be found in literature (Ramirez *et al.* 2000, FEMA 273 1997, FEMA 274 1997, FEMA 450 2003). The terms ξ_{ve} and α are the supplemental damping for a linear structural response and the exponent of velocity of the dampers, respectively.

From Eq. (2), it is evident that the effective damping depends on the displacement, or ductility demand. Therefore, given the supplemental damping ratio under elastic structural response, a series of iterations must be carried out to determine the displacement demand, since the reduced demand spectrum depends upon the effective damping, which, in turn, is related to the displacement, or ductility demand. The assumed supplemental damping ratio is able to satisfy the design objective if the displacement demand is lower than the displacement limit corresponding to the required level of performance. Some of the authors of the present study (Landi *et al.* 2014) proposed an original and direct procedure to determine the minimum supplemental damping ratio that must be provided in order to obtain a given performance. This procedure can be used in combination with the process proposed in the present study for asymmetric-plan structures, as a first step in the design in which the required damping ratio is specified.

3. Design procedure for nonlinear viscous dampers and distribution methods of the damping coefficients

Once the supplemental damping for the seismic retrofit has been fixed and the roof displacement is determined, the subsequent step involves dimensioning the single devices to ensure the desired supplemental damping. Two different methods for obtaining the damping coefficients were considered for this purpose. The first is a simplified method, and considers the structure as a symmetric-plan building in both its principal directions, while ignoring, for the first mode in the direction of the seismic action, the components of rotation and of translation in the orthogonal direction. The second is, instead, an extended method, and considers the structure as an asymmetric plan building and, for the first mode in the direction of the seismic action, takes into account all the components, i.e. the translations along the two principal directions of the buildings as well as the floor rotations. For spatial structures the floor diaphragms are assumed to be rigid.

3.1 Determination of varying damping coefficients for 3D structures

Considering the simplified method, if a 3D symmetric-plan structure is examined, the fundamental mode only involves translations along the direction of the seismic action, therefore the relationships developed for plane frames can be used to study different damping coefficient distributions (Landi *et al*. 2013, Landi *et al.* 2015). According to the design framework being considered (Ramirez *et al*. 2000), the supplemental damping ratio for the first mode of vibration in the direction of the seismic action can be expressed by the following relationship

$$\xi_{ve1} = \frac{\sum_{j=1}^{N_D} (2\pi)^{\alpha_j} T_{e1}^{2-\alpha_j} \lambda_j C_{Nj} f_j^{1+\alpha_j} D_{roof}^{\alpha_j - 1} \Phi_{rj1}^{1+\alpha_j}}{8\pi^3 \sum_{i=1}^{N} m_i \, \Phi_{i1}^2} \tag{3}$$

where N_D and N are the number of dampers and degrees of freedom, respectively, T_{e1} is the elastic period of the first mode in the direction of the seismic action, λ_j is a function of the exponent of the velocity, C_{Nj} is the coefficient of the damper j, f_j is a displacement magnification factor that depends on the geometrical arrangement of the damper, Φ_{rj1} is the difference between the modal ordinates associated with the degrees of freedom connected by means of the damper, Φ_{i1} and m_i are the modal ordinate and the mass of the degree of freedom i, respectively. In addition, D_{roof} is the roof displacement, which is known after applying the procedure described in the previous section.

The distribution of the damping properties can then be defined in the same way as for the plane frames, assuming that the damping coefficient is proportional to a generic parameter γ_j, which is representative of the storey and the frame where the damper is located

$$C_{Nj} = p \;\; \gamma_j \tag{4}$$

where p is a constant to be determined. As illustrated in the case of the plane frames, after several mathematical elaborations, it is possible to obtain an expression for the coefficient of the damper j. Taking the same value of the exponent of the velocity α for all the dampers and assuming that the seismic action is in the x-direction, the following relationship can be used to determine the damping coefficients

$$C_{Njx} = \xi_{ve1} \frac{\gamma_{jx} 8\pi^3 \sum_{i=1}^{N} m_i \Phi_{ix,1x}^2}{(2\pi)^{\alpha} T_{e,1x}^{2-\alpha} \lambda D_{roof,1x}^{\alpha-1} \sum_{j=1}^{N_{Dx}} \gamma_{jx} f_{jx}^{1+\alpha} \, \Phi_{rjx,1x}^{1+\alpha}} \tag{5}$$

where the subscript "1x" identifies the first mode of vibration in the x-direction, which is the mode that activates the greater percentage of mass in this direction. The subscript "x" represents the considered direction. Among the terms described previously, those with subscript "x" assume the same meaning but they are related to quantities, as displacement components or properties of dampers, evaluated along x-direction.

The extended method takes into account all the components of the fundamental mode, which in general is defined by the translations in two orthogonal directions and by the rotation at each floor. For this reason, this leads to the activation not only of the dampers parallel to the direction of the seismic action, but also to those in the orthogonal direction, if any are present. The extended method makes use of different expressions depending on whether the structure presents asymmetry only in one direction or in both principal directions. The general case where the structure is asymmetric in both the directions is initially explained, and a two-equation system so obtained. The method to be used for a structure that presents asymmetry only in one direction is illustrated at a later stage, leading to two equations that can be solved independently.

If the structure has an asymmetric plan in both directions, the viscous damping ratio can be expressed from the following relation containing the parameters associated with the dampers in the two principal directions. The relationships can be written considering the seismic action in the x-direction and assuming that the exponent of velocity α has the same value for all the dampers.

$$\xi_{ve1} = \left[(2\pi)^{\alpha} T_{e,1x}^{2-\alpha} \lambda D_{roof,1x}^{\alpha-1}\right] \cdot \frac{\left[\sum_{j=1}^{N_{Dx}} C_{Njx} f_{jx}^{1+\alpha} \Phi_{rjx,1x}^{1+\alpha} + \sum_{j=1}^{N_{Dy}} C_{Njy} f_{jy}^{1+\alpha} \Phi_{rjy,1x}^{1+\alpha}\right]}{8\pi^3 \left[\sum_{i=1}^{N} m_i \Phi_{ix,1x}^2 + \sum_{i=1}^{N} m_i \Phi_{iy,1x}^2 + \sum_{i=1}^{N} I_i \Phi_{i\theta,1x}^2\right]} \tag{6}$$

where C_{Njx} and C_{Njy} are the damping coefficients of the devices placed in the x and y directions, respectively. N_{Dx} and N_{Dy} are the number of dampers in the x and y directions, considering all the storeys and frames in the respective directions. In addition, the terms $\Phi_{ix,1x}$, $\Phi_{iy,1x}$ and $\Phi_{i\theta,1x}$ are the components of the translation in both the principal directions and the in-plan rotation of the first mode in the direction of the seismic action, which is assumed to be applied in the x-direction. Lastly, I_i represents the polar moment of inertia of the floor mass m_i, whereas the terms $\Phi_{rjx,1x}$ and $\Phi_{rjy,1x}$ represent the inter-story modal deformations evaluated for the first mode in the x-direction and associated to the damper j aligned to the direction x or y, respectively.

The following steps should be then performed to obtain the expressions of the damping coefficients for the extended method. Similarly to the symmetric-plan structures, the damping coefficients are assumed to be proportional to a generic parameter that is typical of the frame and storey where the damper is inserted

$$C_{Njx} = p_x \;\; \gamma_{jx} \tag{7}$$

$$C_{Njy} = p_y \;\; \gamma_{jy} \tag{8}$$

where p_x and p_y are two constants to be determined. By substituting Eqs. (7) and (8) in Eq. (6), the following relationship can be obtained, where the constants p_x and

p_y, at the first member, are the only two unknowns of the problem

$$p_x \sum_{j=1}^{N_{Dx}} \gamma_{jx} f_{jx}^{1+\alpha} \Phi_{rjx,1x}^{1+\alpha} + p_y \sum_{j=1}^{N_{Dy}} \gamma_{jy} f_{jy}^{1+\alpha} \Phi_{rjy,1x}^{1+\alpha} = \\ = \frac{\xi_{ve1} 8\pi^3 \left[\sum_{i=1}^{N} m_i \Phi_{ix,1x}^2 + \sum_{i=1}^{N} m_i \Phi_{iy,1x}^2 + \sum_{i=1}^{N} I_i \Phi_{i\theta,1x}^2\right]}{\left[(2\pi)^\alpha T_{e,1x}^{2-\alpha} \lambda D_{roof,1x}^{\alpha-1}\right]} \tag{9}$$

Similarly, it is possible to obtain another relationship relative to the *y*-direction

$$p_x \sum_{j=1}^{N_{Dx}} \gamma_{jx} f_{jx}^{1+\alpha} \Phi_{rjx,1y}^{1+\alpha} + p_y \sum_{j=1}^{N_{Dy}} \gamma_{jy} f_{jy}^{1+\alpha} \Phi_{rjy,1y}^{1+\alpha} = \\ = \frac{\xi_{ve1} 8\pi^3 \left[\sum_{i=1}^{N} m_i \Phi_{ix,1y}^2 + \sum_{i=1}^{N} m_i \Phi_{iy,1y}^2 + \sum_{i=1}^{N} I_i \Phi_{i\theta,1y}^2\right]}{\left[(2\pi)^\alpha T_{e,1y}^{2-\alpha} \lambda D_{roof,1y}^{\alpha-1}\right]} \tag{10}$$

where the terms $\Phi_{rjx,1y}$ and $\Phi_{rjy,1y}$ represent the inter-storey modal deformations evaluated for the first mode in the *y*-direction relative to the damper *j* installed in the *x* or *y* direction, respectively. In this way, the damping coefficients are obtained from a two-equation system, one associated with a seismic action in the *x*-direction (Eq. (9)), the other considering the seismic action in the *y*-direction (Eq. (10)).

In these equations the intensity and the characteristics of the seismic action affect the term D_{roof}, which is determined with the procedure described in Section 2. In presence of a bidirectional seismic excitation, Eqs. (9) and (10) do not change and the only term which can be affected is D_{roof}. In this case the design can be performed calculating D_{roof} in Eq. (9) by applying the principal component in *x*-direction and D_{roof} in Eq. (10) with the principal component in *y*-direction.

According to the design procedure described above, it is possible to investigate different in-plan and vertical distributions of the damping coefficients, considering the proportionality parameters associated with the storeys and frames in both the principal directions. In previous research carried out by some of the authors, only the uniform distribution was studied within an asymmetric-plan structure (Landi *et al.* 2013). It should be noticed that Eqs. (9) and (10) can be used to dimension the damping coefficients taking a single mode in each direction, in this case the first mode, assuming that it is predominant over the higher modes.

If the structure is asymmetric for seismic action in one direction only, for example *y*-direction, the modal deformation of the first mode in the *x*-direction has no components in the orthogonal direction (i.e., in the *y*-direction) and for the in-plan rotation. In this case, the dampers in the orthogonal direction are not activated and the constant p_y does not appear in the relation for the *x*-direction (Eq. (9)), which has the constant p_x as only unknown quantity and can be solved directly. By obtaining the constant p_x from Eq. (9) and substituting this constant in Eq. (7), it is possible to obtain exactly the Eq. (5). An independent expression for the coefficients C_{Njy} can be also obtained. Once the constant p_x has been derived from Eq. (9), its expression can be inserted into Eq. (10) to obtain the constant p_y. This constant can then be used in Eq. (8). After some mathematical developments, the relationship for the coefficients C_{Njy} can be derived

$$C_{Njy} = \frac{\gamma_{jy} \xi_{ve1} 8\pi^3}{(2\pi)^\alpha \lambda \sum_{j=1}^{N_{Dy}} \gamma_{jy} f_{jy}^{1+\alpha} \Phi_{rjy,1y}^{1+\alpha}} \cdot \\ \cdot \left[\frac{\left[\sum_{i=1}^{N} m_i \Phi_{ix,1y}^2 + \sum_{i=1}^{N} m_i \Phi_{iy,1y}^2 + \sum_{i=1}^{N} I_i \Phi_{i\theta,1y}^2\right]}{\left[T_{e,1y}^{2-\alpha} D_{roof,1y}^{\alpha-1}\right]} - \frac{\left[\sum_{i=1}^{N} m_i \Phi_{ix,1x}^2\right] \sum_{j=1}^{N_{Dx}} \gamma_{jx} f_{jx}^{1+\alpha} \Phi_{rjx,1y}^{1+\alpha}}{\left[T_{e,1x}^{2-\alpha} D_{roof,1x}^{\alpha-1}\right] \sum_{j=1}^{N_{Dx}} \gamma_{jx} f_{jx}^{1+\alpha} \Phi_{rjx,1x}^{1+\alpha}}\right] \tag{11}$$

It is evident that Eq. (11) is more complex than Eq. (5). Eq. (11) contains the translational components along *x*, *y* and the rotational component of the first mode in the *y*-direction, the component along *x*-direction of the first mode in *x*-direction, the inter-story modal deformations $\Phi_{rjx,1x}$, $\Phi_{rjx,1y}$ and $\Phi_{rjy,1y}$, and the proportionality parameters γ_{jx} and γ_{jy}. All the terms in Eq. (11) can be evaluated once the masses of the system, the modal deformations, the viscous damping ratio, the exponent of velocity for the dampers and the roof displacements for the two principal directions are all known. Therefore, on examining a structure with asymmetry for the seismic action in only one of the two principal directions, Eq. (5) can be used to determine the damping coefficients for the direction where the structure is symmetric, Eq. (11) can be used directly to obtain the coefficients for the dampers positioned in the other direction.

3.2 Distribution methods for the damping coefficients in 3D structures

This paragraph shows the extension of the proportionality parameters γ_{jx} or γ_{jy} for 3D structures and for the extended method. In the following expressions the dampers are assumed to be arranged in the direction *x*. Obviously, similar relationships can be written for dampers aligned in *y*-direction. The expressions for the simplified method, which neglects the plan-symmetry, can be obtained by the following ones assuming only translation parallel to seismic action for the modal deformations (a unique value for each storey) and considering the in-plan eccentricity $e_s = 0$.

a) ->Uniform Distribution (UD)

$$\gamma_{jx} = \gamma_{jy} = 1 \tag{12}$$

This distribution, where the parameter γ_{jx} is equal to 1, gives identical coefficients C_{Nj} for all the dampers. It should be noted that the coefficients for the two directions could have different values.

b) -> Mass Proportional Distribution (MPD)

$$\gamma_{jx} = m_j \rho_{jx} = m_j \left(\frac{k_{fjx}}{k_{sjx}} + \frac{e_s k_{fjx} d_{jy}}{\sum_{k=1}^{N_{Tf}} (k_{fjk} d_k^2)} \right) \tag{13}$$

where m_j is the mass at the storey where the damper *j* is installed, and is distributed in the same way as the inertia forces, that is, as a function of the stiffness of the storey and the frame where the damper is positioned. The terms k_{fjx} and k_{sjx} represent the storey stiffness in the *x*-direction of the frame where the damper j is installed, and the storey stiffness in the *x*-direction of all the frames, respectively. On the basis of the characteristics of the structures under study, it is possible to evaluate these storey stiffness considering the frames to have a shear-type behaviour. In addition, d_{jy} represents the distance from the frame where the damper j is arranged to the storey stiffness centre (Fig. 1), while N_{Tf} is the total number of frames at the storey of damper j. In Eq. (13), the coefficient ρ_{jx} represents the portion of floor mass associated to the frame where the device j is installed. Using this coefficient, the mass of the storey is distributed as a function of the stiffness of the frame and the floor where the damper j is positioned, including the floor rotation contribution, which is not considered in the simplified method.

c) -> Storey Stiffness Proportional Distribution (STPD)

$$\gamma_{jx} = k_{fjx} \tag{14}$$

In this distribution, the proportionality parameter of the damper j is equal to the storey stiffness of the frame where the damper is located. This proportionality coefficient does not change passing from the simplified to the extended method, since the storey stiffness of the single frame where the device is inserted is defined with only the translational contribution being considered.

d) -> Storey Shear Proportional Distribution (SSPD)

$$\gamma_{jx} = S_{j,1x}\ \rho_{jx} = \left(\sum_{i=j}^{N} m_i \Phi_{ix,1x}\right) \cdot \left(\frac{k_{fjx}}{k_{sjx}} + \frac{e_s k_{fjx} d_{jy}}{\sum_{k=1}^{N_{Tf}} (k_{fjk} d_k^2)}\right) \tag{15}$$

Here, the proportionality parameter of the damper j is equal to the product of the storey shear at the floor where the damper j is installed and the same stiffness ratio used in the expression for the mass proportional distribution. The storey shear associated to the mode 1*x* at the floor where the damper j is installed, $S_{j,1x}$, is evaluated taking the same lateral force distribution used in the pushover analysis in the *x*-direction, where the lateral force applied at each storey is proportional to the product of the mass and the component in the *x*-direction of the first mode in the *x*-direction.

e) -> Inter-storey Drift Proportional Distribution (IDPD)

$$\gamma_{jx} = D_{roof,1x}\ (\Phi_{rjx,1x}) \tag{16}$$

This distribution provides a proportionality parameter equal to the inter-storey drift at the storey where the damper j is installed, determined on the basis of the first mode deformations in the direction of the damper. These deformations account also for the contribution of floor rotation.

f) -> Shear strain Energy Proportional Distribution (SEPD) and Shear strain Energy Efficient Storeys Proportional Distribution (SEESPD)

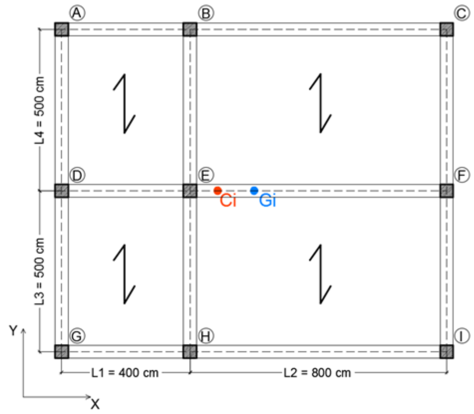

Fig. 1 Plan of the 3D-building (span length in cm)

$$\gamma_{jx} = S_{j,1x}\ \rho_{jx} D_{roof,1x}\ (\Phi_{rjx,1x}) = \left(\sum_{i=j}^{N} m_i \Phi_{ix,1x}\right)\left(\frac{k_{fjx}}{k_{sjx}} + \frac{e_s k_{fjx} d_{jy}}{\sum_{k=1}^{N_{Tf}} (k_{fjk} d_k^2)}\right) \cdot D_{roof,1x}\ (\Phi_{rjx,1x}) \tag{17}$$

For each damper j, the proportionality parameters associated to the proportional distribution of shear strain energy (SEPD) and the proportional distribution of shear strain energy in efficient storeys (SEESPD), which are two energy methods proposed in literature (Hwang *et al*. 2013), is obtained as the product of the inter-story drift given by Eq. (16), with the storey shear given by Eq. (15) relative to the floor and the frame where the damper is installed.

In the SEESPD distribution, the dampers are only distributed on the efficient storeys, defined as the storeys where the shear strain energy is greater than the average shear strain energy (Hwang *et al*. 2013), evaluated considering all the storeys and frames in the *x*-direction. Looking specifically at the dampers in the *x*-direction, the following condition can be obtained

$$S_{j,1x}\ \rho_{jx}(\Phi_{rjx,1x}) > \frac{\sum_{j=1}^{N_{Dx}} S_{j,1x}\ \rho_{jx}\ (\Phi_{rjx,1x})}{N_{Dx}} \tag{18}$$

where N_{Dx} is the total number of dampers arranged in the *x*-direction considering all the frames and storeys in the structure.

It should be noted that, for a single plane frame, the proportionality parameters depends on the properties of the storey where the damper is inserted, while for a three-dimensional structure, it is connected to the position where the damper is placed and can vary in the same storey from frame to frame. In this case, the proportionality parameter depends on the properties of the storey and frame where the device is positioned.

4. Case study

The asymmetric building examined in this study is a six-floor RC frame building (Fig. 1) measuring, in-plan, 10 m in the *y*-direction and 12 m in the *x*-direction. The in-plan

Table 1 Cross-section dimensions for columns and beams (width×depth in cm)

STOREY	COLUMNS						BEAMS		
	A-G	B-H	C-I	D	E	F	ABC-GHI	DEF	ADG-BEH-GHI
storey 6	30×30	35×35	30×30	30×30	35×35	30×30	30×40	35×45	30×40
storey 5	30×30	35×35	30×30	30×30	35×35	30×30	30×45	35×50	30×40
storey 4	30×30	35×35	30×30	35×35	40×40	35×35	30×45	35×50	30×40
storey 3	30×30	35×35	30×30	35×35	40×40	35×35	30×45	35×50	30×40
storey 2	35×35	40×40	35×35	40×40	45×45	40×40	30×45	35×50	30×40
storey 1	35×35	40×40	35×35	40×40	45×45	40×40	30×45	35×50	30×40

Table 2 Dynamic properties of each mode

MODE	T_e [s]	M_x [%]	M_y [%]	M_ϑ [%]
1Y	1.36	0%	68%	12%
1R	1.18	0%	12%	68%
1X	1.17	80%	0%	0%
2Y	0.46	0%	9%	2%
2X	0.41	11%	0%	0%
2R	0.40	0%	2%	9%

eccentricity is about 1 m along the *x*-direction on each floor. The inter-storey is 3.3 m in height at each storey. The columns of square cross-section vary in size depending on the storey and frame being considered (Table 1). It was assumed that the structure had been designed for gravity loads for a building in a site only classified as a seismic zone after its construction. The total floor weight is equal to 981 kN at the roof and to 1492 kN at all intermediate levels. The mechanical properties of materials are assumed as follows: the mean concrete cylinder strength is equal to 28 MPa and steel yield strength is equal to 450 MPa.

The modal analysis, performed using a finite element computer program (CSI 2009), provided the modal shapes and other dynamic properties of the structure, such as the elastic period T_e and the effective modal masses (M_x, M_y and M_ϑ) for each mode. The modes were ordered in triplets, according to the main direction along which masses are activated in each mode (Table 2).

In the nonlinear analyses, the structural elements were modelled by adopting a concentrated plasticity model, which was implemented in the same finite element computer program noted above. The plastic hinges were located at the ends of each element (columns and beams) and were defined by a bilinear moment-rotation curve. The yielding rotation (ϑ_y), the rotation capacities associated to the damage limitation (ϑ_{DL}) and the collapse prevention limit states (ϑ_{CP}) were all determined using the empirical relationships set out in the Italian Building Code (NTC 2008, Istruzioni NTC 2009) and inspired by the formulae proposed by Panagiotakos and Fardis (Panagiotakos and Fardis 2001). According to the Italian guidelines (Istruzioni NTC 2009), the rotation associated to the life safety limit state (ϑ_{LS}) was set equal to 75% of that associated to the collapse limit state.

The nonlinear static analysis was performed by adopting a lateral load distribution referred to as a modal pattern, and was obtained by applying lateral forces at each floor proportional to the storey masses multiplied by the corresponding modal deformations of the dominant mode in

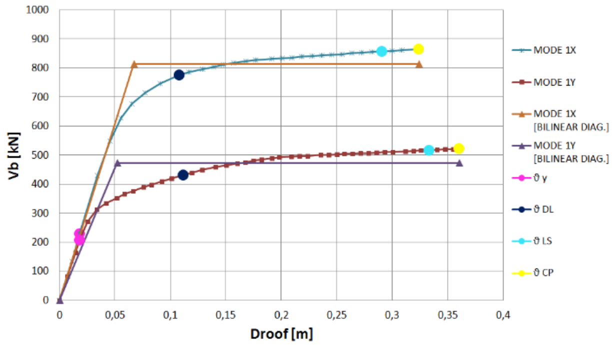

Fig. 2 Pushover curves and elastic-perfectly plastic idealizations

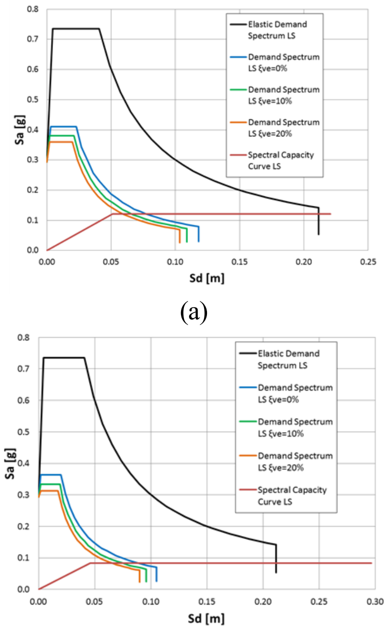

(a)

(b)

Fig. 3 Performance points in the spectral acceleration-spectral displacement (S_a-S_d) plane in the *y*-direction (a) and in the *x*-direction (b)

the direction of the seismic action. The pushover curves obtained for both the *x*-direction and the *y*-direction are shown in Fig. 2, which also shows the points associated to the attainment of the different limit states in terms of chord rotations. The pushover curves were idealized through an elastic-perfectly plastic diagram with an elastic branch that passes through the point associated to 60% of the maximum base shear, and with a plastic branch such that the area

Table 3 Damping coefficients in the x-direction determined through the simplified and extended methods: ξ_{ve1} equal to 10% (left) or to 20% (right)

DAMPER	$CNjx$ [kN(s/m)$^{0.5}$] – SIMPLIFIED AND EXTENDED METHOD													
	ξ_{ve1}=10%							ξ_{ve1}=20%						
	UD	MPD	STPD	SSPD	IDPD	SEPD	SEESPD	UD	MPD	STPD	SSPD	IDPD	SEPD	SEESPD
6AB	304	203	199	74	111	26	0	575	383	376	140	210	50	0
5AB	304	309	199	179	236	134	0	575	583	376	338	445	253	0
4AB	304	245	199	212	308	208	0	575	463	376	401	582	393	0
3AB	304	245	199	265	383	322	412	575	463	376	500	723	608	779
2AB	304	253	354	306	326	317	405	575	478	670	578	615	598	766
1AB	304	253	354	319	228	232	0	575	478	670	603	432	438	0
6DE	304	203	199	74	111	26	0	575	383	376	140	210	50	0
5DE	304	309	199	179	236	134	0	575	583	376	338	445	253	0
4DE	304	436	354	378	308	370	474	575	825	670	714	582	700	896
3DE	304	436	354	472	383	574	735	575	825	670	892	723	1084	1388
2DE	304	420	588	507	326	525	672	575	793	1110	958	615	992	1270
1DE	304	420	588	529	228	384	492	575	793	1110	1000	432	726	930
6GH	304	203	199	74	111	26	0	575	383	376	140	210	50	0
5GH	304	309	199	179	236	134	0	575	583	376	338	445	253	0
4GH	304	245	199	212	308	208	0	575	463	376	401	582	393	0
3GH	304	245	199	265	383	322	412	575	463	376	500	723	608	779
2GH	304	253	354	306	326	317	405	575	478	670	578	615	598	766
1GH	304	253	354	319	228	232	0	575	478	670	603	432	438	0
∑TOTx	5475	5240	5290	4851	4776	4491	4009	10344	9900	9995	9165	9023	8486	7574
ΔUD	/	-4.3%	-3.4%	-11.4%	-12.8%	-18.0%	-26.8%	/	-4.3%	-3.4%	-11.4%	-12.8%	-18.0%	-26.8%

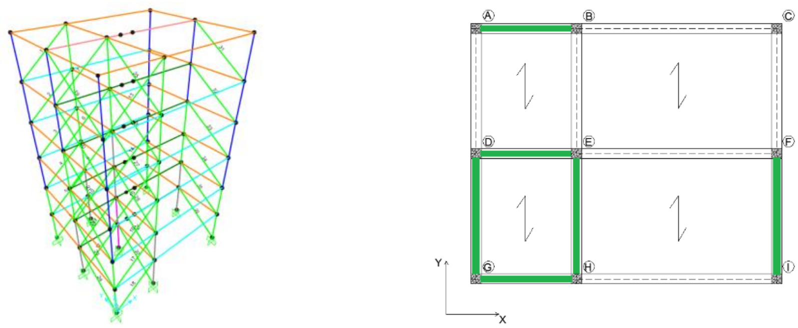

(a) (b)

Fig. 4 Damper positions in the finite element 3D model (a) and in the plane (b)

under the idealized curve is equal to the area under the pushover curve (Istruzioni NTC 2009).

4.1 Design of the damping system

The design procedure for the damping system was applied with reference to the Life Safety limit state (LS). The idealized elastic-perfectly plastic diagrams were then converted into spectral coordinates and superimposed on the demand spectrum (Fig. 3). The elastic demand spectrum was defined under the specifications in the Italian Building Code (NTC 2008), assuming that the 3D-building examined is located in a site where the reference peak ground acceleration is 0.293 g for the life safety limit state and that the soil is of type C. Given the spectral capacity curves for both directions of the seismic action and the reduced demand spectrum for an inherent damping ratio of 5%, it was possible to apply the procedure described in section 2 to determine the seismic demand for the bare structure (supplemental damping ratio ξ_{ve1} =0%). The procedure wasthen applied considering the addition of supplemental dampers to reduce the seismic demand for the considered limit state. The exponent α of velocity in the force-velocity law of the dampers was assumed to be 0.5. Regarding this choice, the motivation was the need of focusing the numerical enquiry on an average value of the range of variation (0.1-1) of this parameter. The previous study (Landi *et al*. 2015) which examined different vertical distributions of damping coefficients for plane frames, considered also case studies with different values of the exponent α, in particular 0.5 and 0.2. In the mentioned study the effect of this variation of the damping exponent was examined in detail. In particular, the differences observed for the design parameters between the different distribution methods were similar for the two values of α.

The damping system was designed twice, applying two different values for the supplemental damping ratio (ξ_{ve1}) under elastic structural response, i.e., 10% and 20% for both

Table 4 Damping coefficients in the y-direction: simplified method, $\boldsymbol{\xi_{ve1}}$ equal to 10% (left) or to 20% (right)

CNjy [kN(s/m)$^{0.5}$] – SIMPLIFIED METHOD														
DAMPER	ξ_{ve1}=10%							ξ_{ve1}=20%						
	UD	MPD	STPD	SSPD	IDPD	SEPD	SEESPD	UD	MPD	STPD	SSPD	IDPD	SEPD	SEESPD
6AB	220	114	112	42	80	15	0	412	214	210	79	151	28	0
5AB	220	174	112	101	170	76	0	412	326	210	190	319	142	0
4AB	220	177	144	154	223	151	0	412	332	270	288	419	283	0
3AB	220	177	144	192	275	231	294	412	332	270	360	516	435	552
2AB	220	183	256	221	239	233	296	412	343	481	415	449	437	555
1AB	220	183	256	230	155	157	0	412	343	481	433	291	295	0
6DE	220	211	207	78	80	27	0	412	397	390	146	151	51	0
5DE	220	322	207	187	170	140	0	412	604	390	352	319	263	0
4DE	220	315	256	274	223	268	341	412	592	481	514	419	504	640
3DE	220	315	256	341	275	413	523	412	592	481	641	516	775	983
2DE	220	303	425	367	239	386	490	412	569	798	689	449	725	920
1DE	220	303	425	382	155	261	331	412	569	798	717	291	490	621
6GH	220	114	112	42	80	15	0	412	214	210	79	151	28	0
5GH	220	174	112	101	170	76	0	412	326	210	190	319	142	0
4GH	220	177	144	154	223	151	0	412	332	270	288	419	283	0
3GH	220	177	144	192	275	231	294	412	332	270	360	516	435	552
2GH	220	183	256	221	239	233	296	412	343	481	415	449	437	555
1GH	220	183	256	230	155	157	0	412	343	481	433	291	295	0
∑TOTy	3952	3782	3825	3507	3425	3220	2863	7422	7105	7184	6588	6434	6048	5378
ΔUDs	/	-4.3%	-3.2%	-11.2%	-13.3%	-18.5%	-27.5%	/	-4.3%	-3.2%	-11.2%	-13.3%	-18.5%	-27.5%

Table 5 Damping coefficients in the y-direction: extended method, ξ_{ve1} equal to 10% (left) or to 20% (right)

CNjy [kN(s/m)$^{0.5}$] – EXTENDED METHOD														
DAMPER	ξ_{ve1}=10%							ξ_{ve1}=20%						
	UD	MPD	STPD	SSPD	IDPD	SEPD	SEESPD	UD	MPD	STPD	SSPD	IDPD	SEPD	SEESPD
6AB	210	95	114	35	40	7	0	393	178	214	65	76	12	0
5AB	210	145	114	84	84	33	0	393	271	214	158	157	62	0
4AB	210	146	147	126	107	63	0	393	273	275	237	202	119	0
3AB	210	146	147	158	131	96	0	393	273	275	296	246	181	0
2AB	210	152	262	184	118	101	0	393	285	491	346	222	190	0
1AB	210	152	262	192	72	64	0	393	285	491	360	135	120	0
6DE	210	198	212	72	58	20	0	393	371	397	136	109	37	0
5DE	210	300	212	175	122	100	0	393	564	397	328	230	187	0
4DE	210	294	262	255	160	190	219	393	551	491	479	300	356	411
3DE	210	294	262	318	197	291	336	393	551	491	598	369	546	630
2DE	210	283	434	342	173	275	317	393	531	814	643	324	516	595
1DE	210	283	434	357	110	183	211	393	531	814	669	207	343	396
6GH	210	130	114	48	93	21	0	393	244	214	89	175	39	0
5GH	210	197	114	115	200	107	0	393	371	214	216	375	200	0
4GH	210	203	147	177	265	218	251	393	381	275	332	497	408	471
3GH	210	203	147	220	327	335	387	393	381	275	414	614	630	726
2GH	210	208	262	251	281	329	379	393	390	491	472	528	617	712
1GH	210	208	262	262	187	228	263	393	390	491	491	352	428	494
∑TOTy	3772	3634	3905	3373	2727	2659	2363	7077	6820	7328	6329	5117	4991	4435
ΔUDe	/	-3.6%	3.5%	-10.6%	-27.7%	-29.5%	-37.4%	/	-3.6%	3.5%	-10.6%	-27.7%	-29.5%	-37.4%
ΔUDs	-4.6%	-8.1%	-1.2%	-14.7%	-31.0%	-32.7%	-40.2%	-4.6%	-8.1%	-1.2%	-14.7%	-31.0%	-32.7%	-40.2%

the principal directions. These supplemental damping ratio values do not exceed the maximum reduction of the spectral ordinates allowed in the different guidelines or codes, such as the Italian Building Code and Eurocode 8 (NTC 2008, Eurocode 8 2003).

Using the known seismic demand in terms of spectral displacement, it was possible to derive the seismic demand in terms of roof displacement for each of the six cases given by the two directions and the three values of ξ_{ve1}: 0%, 10% and 20%. Then, in order to achieve the two prefixed values of the supplemental damping ratio, the damping system was designed according to the different methods (simplified or extended) and different distribution criteria (Eqs. (12)-(18)) presented in section 3. The extended method was applied considering that the case study is asymmetric for seismic action in the y-direction, while it is symmetric in the orthogonal direction. With regards to the damper positioning, one damper was inserted in each frame at each floor for all the distributions of the damping coefficients (Fig. 4), except for the SEESPD, which provides dampers only at the levels where the shear strain energy exceeds the average value.

Obviously, the proportionality parameters associated with the dampers in the x-direction are the same for both the simplified or the extended method, due to the symmetry of the building in this direction, whereas the proportionality parameters associated with the dampers in the y-direction differ for the two methods. Similarly, the values of the damping coefficients in the x-direction are the same for both methods (Table 3), while the values of the damping coefficients in the y-direction differ according to the method used (Tables 4 and 5). Tables 3-5 show the damping coefficient of each single damper, and the bottom lines give the sums of all the coefficients and the percent variations towards uniform distribution, assumed as reference, for each method and for all the considered distributions. In Table 5 the percentage variations are evaluated both against the UD with the simplified method (ΔUDs) and the UD with the extended method (ΔUDe).

The structures examined include the bare 3D-building and the building with added dampers to give a 10% and 20% supplemental damping ratio, where, for each damping ratio, the damping system was designed using both the simplified and extended methods, and considering, for each method, the seven damping distributions described previously. In this way, as well as the bare frame, the previously mentioned options lead to 28 different cases each with different damping systems. In addition to these, two further distributions with a 20% supplemental damping ratio were also examined, both of these arising as a version of the SEESPD distribution applied in combination with the extended method. Considering these two further distributions, 31 different cases were examined overall. The reason why these additional two distributions were considered is explained as follows. With ξ_{ve1}=20% and the SEESPD distribution, no dampers were placed in the ADG frame (Table 5), therefore, in order to limit the drifts in such a frame, two further distributions were defined, imposing a further condition on the SEESPD distribution. This condition involved a minimum number of dampers to be inserted in each frame, set at 2 for first additional case, and at 4 for the second. The two corresponding distributions were called SEESPD(2T) and SEESPD(4T), respectively.

The damping coefficients determined according to the different distributions, in general, vary along the plane and height. Those obtained using MPD are almost constant along the height, except at the last storey, but are different for the external and the internal frames.

This is because these coefficients depend on the stiffness of the frames (Eq. (13)), and the columns of the internal frame have larger cross-sections than those of the external frames. The coefficients obtained with the STPD and SSPD distributions increase from the upper to the lower storeys, with larger values at the base given by STPD. According to the stiffness of the columns, the coefficients given by STPD and SSPD (Eqs. (14) and (15)) are larger for the internal frame. As expected, the IDPD distribution provided constant values of the damping coefficients along the plane using the simplified method, and larger values at the intermediate storeys. Looking at the energy methods, the SEPD method gave variable values for the damping coefficients along the plfane and the height, where very low values are at the upper storeys and high values at the intermediate storeys, with the maximum values being at the internal frames. In the SEESPD method, no dampers were distributed at the upper storeys (where the values obtained with SEPD were low) and this was also sometimes the case for the first storey, thus giving larger maximum damping coefficients at the intermediate storeys than when using SEPD. As previously mentioned, when SEESPD is applied with the extended method, no dampers are allocated to the external frame in the y-direction at the stiffer side.

Considering the lower lines in Tables 3-5, if one method produces a reduction in the total sum of the damping coefficients, compared to the UD, this method would give an advantage without expecting strong variations in the structural performance, given that the supplemental damping is the same. The structural performance has, in any case, been verified through nonlinear time-history analyses, as shown in the next section. By changing the supplemental damping ratio, the only parameter that changes in Eqs. (5) and (11), apart from ξ_{ve1}, is the roof displacement. For both equations mentioned, it is possible to deduce that, for a given distribution, the ratio between the damping coefficients obtained with ξ_{ve1}=10% and those derived with ξ_{ve1}=20% is constant for all dampers. This means that the differences in percentage between the different distributions and the UD are independent of the considered supplemental damping.

All the distribution methods determined a benefit compared to the UD, except when STPD is used with the extended method, where the percentage increase was in any case very low, about 3%. The advantage was significant mainly for the energy distribution methods (SEPD and SEESPD). The MPD and STPD distributions with the simplified method produced a modest improvement, less than 5%. The SSPD and IDPD distributions produced a similar improvement of about 11-13% using the simplified method. Between the two energy methods, the reduction of the total damping coefficient compared to the UD is maximized in the case where the dampers are distributed only on the "Efficient Storeys". In this case it is possible to achieve a reduction of about 27% with the simplified method. If the extended rather than the simplified method is used, a further reduction in the total damping coefficient can be obtained for all the distributions except the STPD, where the increase was very low. The reason why the extended method produces a reduction is due to the fact that the evaluation of the supplemental damping ratio takes in the contribution of the dampers in both the x and y directions. The entity of this reduction can be correlated to the degree of coupling between the translational and rotational modes. The reduction observed in the case study involving the extended method was more significant for the IDPD and the energy methods. This reduction calculated against the UD involving the simplified method was between 13% and 31% for the IDPD, between 18% and 32% for the SEPD and between 27% and 40% for the

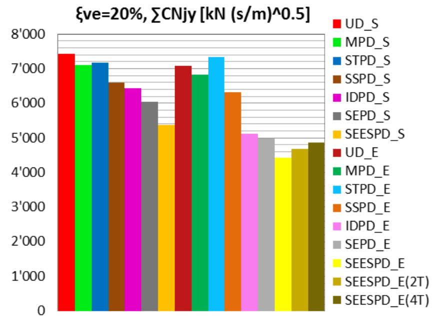

(a)

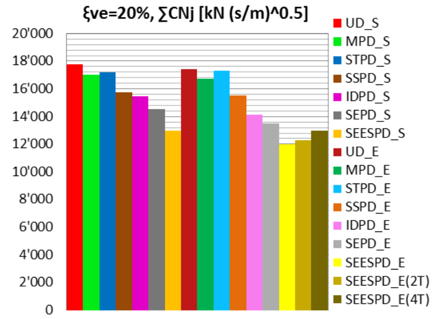

(b)

Fig. 5 Sum of damping coefficients only in the y-direction (a) or in both directions (b), ξ_{ve1}=20%

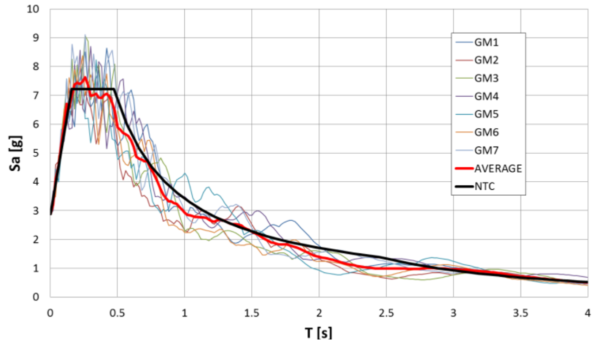

Fig. 6 Spectrum of each ground motion (GM), and comparison between the average spectrum of the seven ground motions (AVERAGE) and the Italian Building Code spectrum (NTC)

SEESPD. Fig. 5 shows, for ξ_{ve1}=20%, the total sum of the damping coefficients only for the dampers in the y-direction (∑$CNjy$) and for those in both directions (∑CNj), meaning that the results of all the case studies can be compared through a synthetic graphic representation, which confirms the trends previously described. The two further distributions SEESPD(2T) and SEESPD(4T), especially the first, did not provide any relevant difference from SEESPD.

4.2 Results of nonlinear time-history analyses

Once the damping coefficients were determined for each device, considering all the distributions, it was possible to perform the nonlinear dynamic analyses for all the 31 different cases. The 3D-building with the different damping distributions was then subjected to a set of seven artificial spectrum-compatible ground motions, obtained by applying SIMQKE software (NISEE 1976). The average spectrum of the seven ground motions under consideration, obtained by means of SeismoSignal 2016 (Seismosoft 2016), is compared with the code elastic spectrum for a 5% damping in Fig. 6. Overall, 217 NLDAs were performed, one time-history analysis for each ground motion and for each of the 31 examined cases. Since the case study is asymmetric for seismic action in y-direction, the nonlinear dynamic analyses were performed by applying the ground motions in y-direction. A simultaneous secondary component in x-direction was not applied because this component would affect the response in the same direction and in order to simplify the interpretation of the results.

The examined response parameters are the maximum inter-storey drifts in the direction of each frame (δ), the residual inter-storey drifts (δ_r, response quantity concerning the reparability of the frame after a major earthquake) and the peak floor accelerations (response quantity concerning acceleration-sensitive non-structural components). In general, it should be noticed that for an asymmetric-plan building also a perpendicular drift component may be present. However, considering that the seismic action was applied in the y direction, the drift component measured along this direction is expected to be predominant, and the results regarding this component are able to provide the

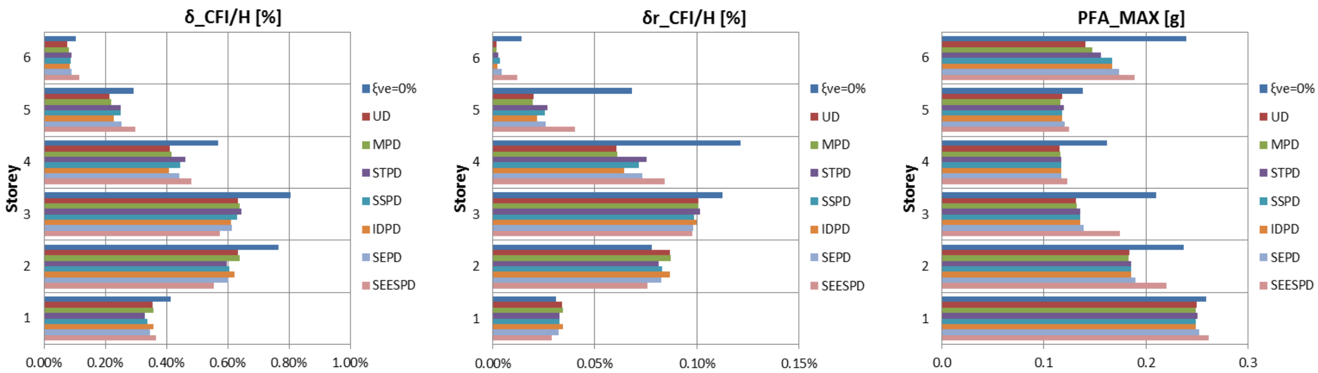

(a) (b) (c)

Fig. 7 Maximum values at each storey of the considered response quantities for the simplified method and ξ_{ve1}=10%

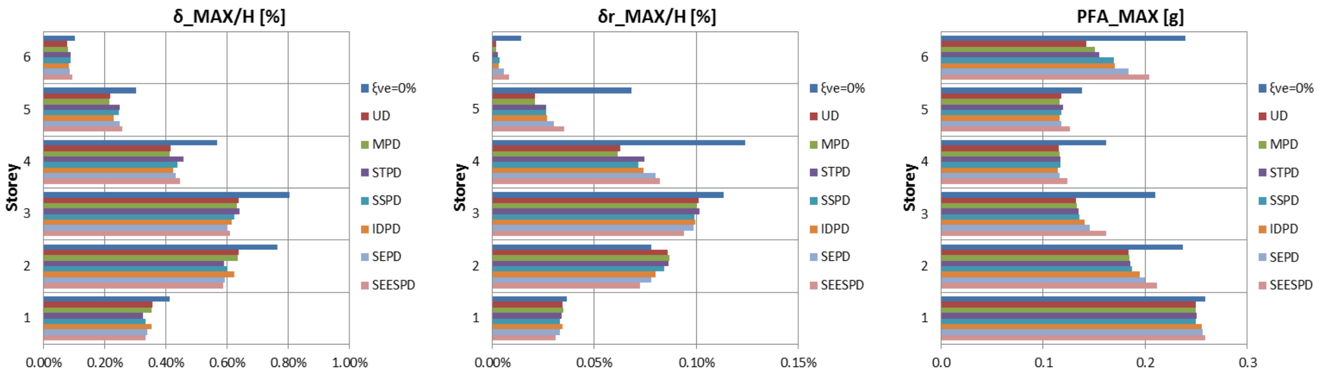

(a) (b) (c)

Fig. 8 Maximum values at each storey of the considered response quantities for the extended method and ξ_{ve1}=10%

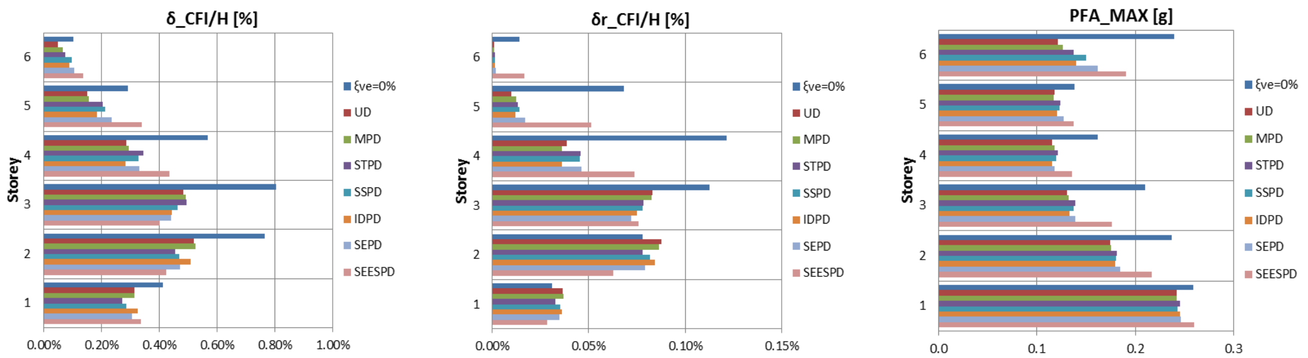

(a) (b) (c)

Fig. 9 Maximum values at each storey of the considered response quantities for the simplified method and ξ_{ve1}=20%

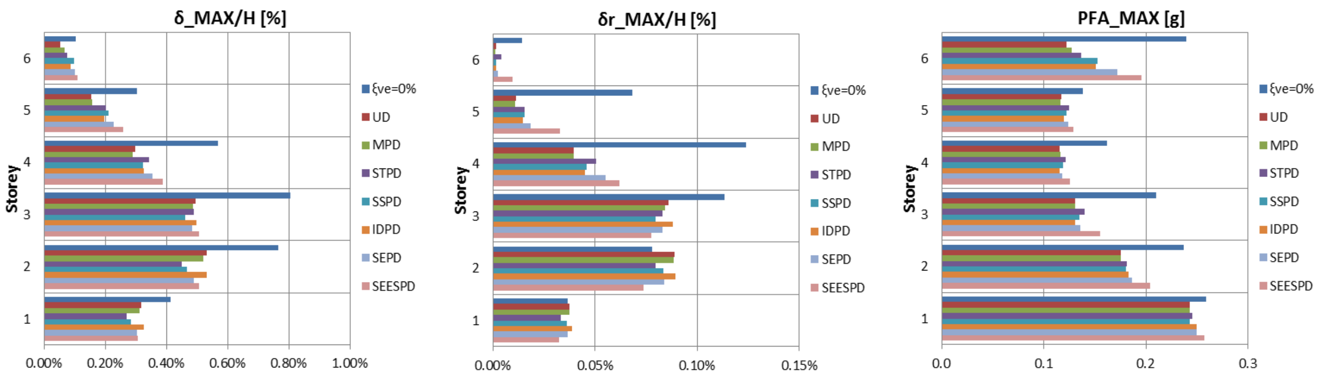

(a) (b) (c)

Fig. 10 Maximum values at each storey of the considered response quantities for the extended method and ξ_{ve1}=20%

trends due to the different distributions of the damping coefficients.

With regards to the dampers, as well as the damping coefficient, the maximum damper force (F_{Dj}) is another significant design parameter relating to the cost, and it affects the forces transmitted to the linked structural elements. This parameter was also determined using the time-history analyses.

Initially, one value for each storey and each frame was determined for the different response quantities in the direction of the corresponding frame. This value was evaluated as the average of the response quantities obtained for each ground motion. This produced masses of data. One value at each floor was, therefore, evaluated using two criteria, where the first involved deriving the maximum value for the three frames in the y-direction (the direction of the seismic action), and the second consisted in calculating the sum of the values for the three times.

The two values were obtained by means of the above two criteria at each floor, for all the considered response quantities: the maximum inter-storey drifts (δ_MAX, $\sum \delta_y$), the residual interstory drifts (δr_MAX, $\sum \delta_{r,y}$) and the peak floor accelerations (PFA_MAX, $\sum PFA_y$). It was then possible to obtain a profile along the height of each

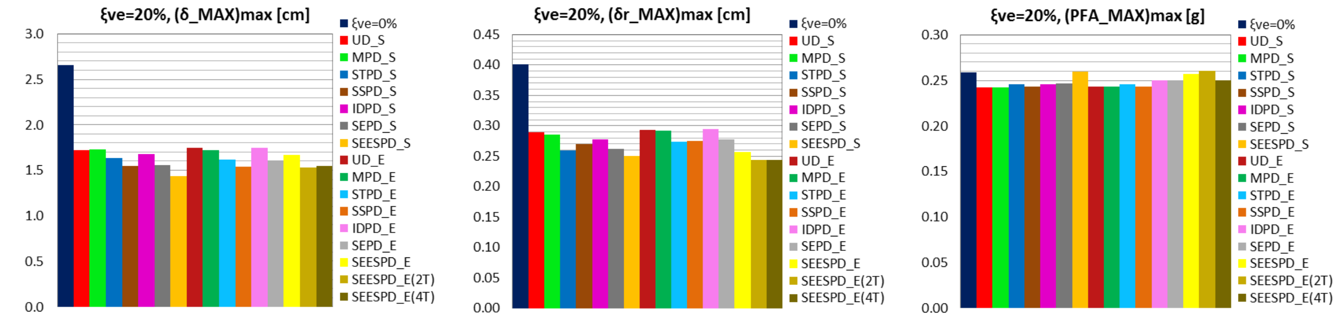

(a) (b) (c)

Fig. 11 Maximum values at each storey of the considered response quantities for the simplified method and ξ_{ve1}=20%

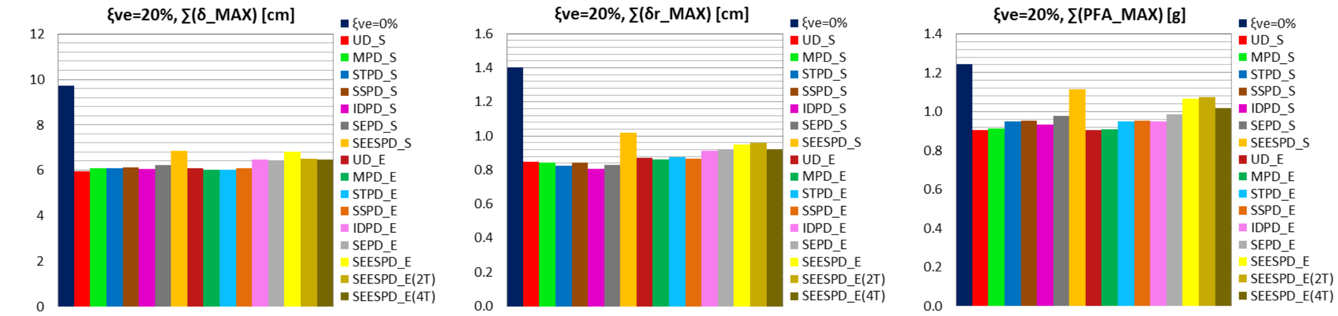

(a) (b) (c)

Fig. 12 Maximum values at each storey of the considered response quantities for the extended method and ξ_{ve1}=20%

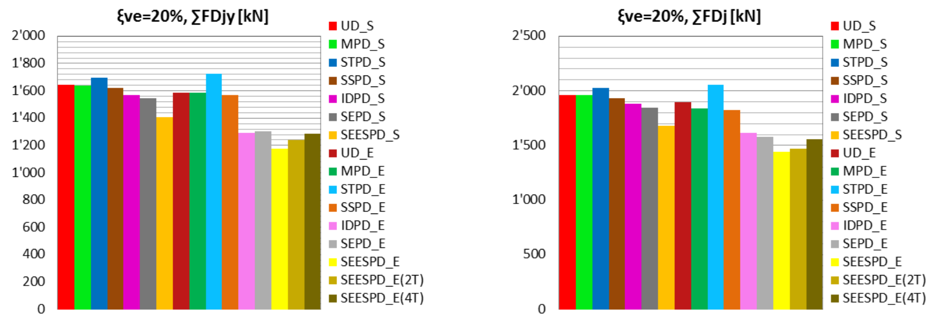

(a) (b)

Fig. 13 Sum of maximum damper forces only in the y-direction (a) or in both directions (b): ξ_{ve1}=20%, simplified and extended methods

response parameter, and the profiles regarding the maximum value at each floor are given in Fig. 7 to Fig. 10 for all cases.

It is possible to observe that, as expected, the reduction of the considered response parameters, in particular of the maximum and residual inter-storey drifts, is greater when ξ_{ve1}=20% than when ξ_{ve1}=10%. From the figures, it can also be seen that the profiles of the response parameters are quite similar for the structures with different distributions of dampers. Given the entity of the reduction provided by the supplemental damping and the maximum values along the height for the structures with added dampers, the differences between the different distributions are not extensive. This result can be explained by considering that the different distributions are compared for the same value of ξ_{ve1}. It should be noted that the SEESPD did not provide any displacement control at the storeys where the dampers were not installed, producing rifts sometimes greater than those of the bare frame, such as in the design with ξ_{ve1}=20% and use of the simplified method (Fig. 9). This result was less evident when the extended method is used. On the other hand, the SEESPD determined a more uniform distribution of the drifts, and the non-controlled storeys showed, in general, low values in drift demand.

Moreover, when compared with the other distribution, in general the SEESPD provided the largest reduction in drifts at the 2nd and 3rd storeys, where the maximum drift demand along the height was obtained. The introduction of dampers also determined a significant reduction of the residual inter-storey drifts, more significant when ξ_{ve1}=20% than when ξ_{ve1}=10%. With regards to the peak floor accelerations, the introduction of dampers produced a more evident reduction

Table 6 Summary parameters for ξ_{ve1}=10%: percentage difference compared to SEESPD with the extended method

	SIMPLIFIED METHOD							*EXTENDED METHOD*						
ξ_{ve1}=10%	UD	MPD	STPD	SSPD	IDPD	SEPD	SEESPD	UD	MPD	STPD	SSPD	IDPD	SEPD	SEESPD
(δ_MAX)max	4%	5%	6%	3%	2%	1%	-6%	5%	4%	5%	2%	3%	-1%	/
∑(δ_MAX)	-1%	1%	1%	1%	-1%	0%	2%	1%	0%	1%	0%	0%	-1%	/
(∑δy)max	-1%	-1%	0%	-3%	-2%	-6%	-12%	1%	0%	-1%	-1%	3%	0%	/
∑(∑δy)	-5%	-5%	-4%	-5%	-5%	-6%	-6%	-4%	-4%	-5%	-4%	0%	-1%	/
(δr_MAX)max	7%	7%	8%	5%	6%	4%	4%	7%	7%	8%	5%	6%	5%	/
∑(δr_MAX)	-6%	-6%	-1%	-3%	-4%	-2%	5%	-5%	-5%	1%	-2%	-2%	1%	/
(∑δr,y)max	7%	7%	9%	5%	6%	5%	4%	7%	7%	8%	5%	6%	5%	/
∑(∑δr,y)	-5%	-5%	0%	-2%	-4%	-1%	5%	-5%	-5%	-1%	-2%	-2%	1%	/
(PFA_MAX)max	-4%	-4%	-3%	-4%	-4%	-3%	1%	-4%	-4%	-3%	-4%	-1%	-1%	/
∑(PFA_MAX)	-14%	-13%	-11%	-11%	-11%	-9%	1%	-13%	-13%	-11%	-10%	-9%	-6%	/
(∑PFA,y)max	-2%	-2%	-2%	-2%	-1%	-1%	3%	-2%	-2%	-2%	-2%	-1%	0%	/
∑(∑PFA,y)	-11%	-10%	-8%	-8%	-8%	-5%	1%	-10%	-10%	-9%	-7%	-7%	-4%	/
∑ CNjy	67%	60%	62%	48%	45%	36%	21%	60%	54%	65%	43%	15%	13%	/
∑ CNj	48%	42%	43%	31%	29%	21%	8%	45%	39%	44%	29%	18%	12%	/
∑ FDjy	47%	44%	48%	40%	36%	32%	21%	41%	39%	51%	35%	11%	11%	/
∑ FDj	49%	45%	48%	40%	39%	33%	19%	44%	38%	51%	34%	17%	13%	/

Table 7 Summary parameters for ξ_{ve1}=20%: percentage difference compared to SEESPD with the extended method

	SIMPLIFIED METHOD							EXTENDED METHOD								
ξ_{ve1}=20%	UD	MPD	STPD	SSPD	IDPD	SEPD	SEES PD	UD	MPD	STPD	SSPD	IDPD	SEPD	SEESPD	SEESPI (2T)	SEESPI (4T)
(δ_MAX)max	3%	4%	-2%	-7%	1%	-7%	-14%	5%	3%	-3%	-8%	5%	-3%	/	-8%	-7%
∑(δ_MAX)	-13%	-11%	-11%	-10%	-11%	-9%	0%	-11%	-12%	-12%	-11%	-5%	-6%	/	-5%	-5%
(∑δy)max	3%	2%	-5%	-9%	0%	-9%	-21%	5%	4%	-6%	-7%	9%	0%	/	-5%	-4%
∑(∑δy)	-13%	-13%	-13%	-13%	-12%	-12%	-7%	-11%	-11%	-14%	-11%	-3%	-3%	/	-2%	-3%
(δr_MAX)max	13%	11%	1%	5%	8%	2%	-3%	14%	14%	7%	7%	15%	8%	/	-5%	-5%
∑(δr_MAX)	-11%	-11%	-13%	-11%	-15%	-12%	7%	-8%	-9%	-8%	-9%	-3%	-3%	/	1%	-3%
(∑δr,y)max	14%	13%	5%	6%	10%	3%	-2%	17%	16%	6%	9%	17%	10%	/	-4%	-3%
∑(∑δr,y)	-8%	-9%	-9%	-10%	-13%	-11%	7%	-6%	-6%	-8%	-6%	-1%	-1%	/	2%	0%
(PFA_MAX)max	-6%	-6%	-4%	-6%	-4%	-4%	1%	-5%	-6%	-4%	-5%	-3%	-3%	/	1%	-3%
∑(PFA_MAX)	-15%	-15%	-11%	-11%	-12%	-8%	5%	-15%	-15%	-11%	-11%	-11%	-8%	/	1%	-4%
(∑PFA,y)max	-4%	-4%	-2%	-4%	-2%	-2%	4%	-3%	-4%	-2%	-3%	-1%	-1%	/	1%	-1%
∑(∑PFA,y)	-12%	-12%	-8%	-7%	-9%	-5%	5%	-12%	-12%	-8%	-7%	-8%	-5%	/	1%	-1%
∑ CNjy	67%	60%	62%	49%	45%	36%	21%	60%	54%	65%	43%	15%	13%	/	6%	10%
∑ CNj	48%	42%	43%	31%	29%	21%	8%	45%	39%	44%	29%	18%	12%	/	2%	8%
∑ FDjy	40%	39%	45%	38%	34%	32%	20%	35%	35%	47%	34%	10%	11%	/	6%	10%
∑ FDj	36%	36%	41%	34%	31%	28%	17%	32%	27%	43%	26%	12%	10%	/	2%	8%

at the intermediate and upper storeys. This reduction was similar for the various distribution methods except for the SEESPD, which provided slightly larger values for the peak floor accelerations. Moving from the simplified to the extended method determined a slight increase of the maximum inter-storey drifts for the IDPD and the energy methods, where the values are slightly larger for the SEESPD (this aspect will be examined in more detail later, and the percentage values will be shown). A point to note is that using the extended method with these distributions provided larger damping coefficients on the flexible side of the frame (CFI), recording, as a consequence, slightly larger drifts than the former on the stiffer side of the frame (ADG).

Summary parameters were also defined and calculated to obtain a single value for each distribution of damping coefficient and also to ease the comparison between the different distributions. This involved examining the maximum value for all the storeys and the total sum of the values derived at each storey for the response parameters evaluated using the two previous mentioned criteria. In this way, four summary parameters were obtained for each response quantity and each distribution. For example, considering the maximum inter-storey drifts, the following four parameters were evaluated: the maximum value of the maximum drift at each storey for all the storeys (δ_MAX)max, the sum of the maximum drift at each storey for all the storeys, $\sum(\delta\_MAX)$, the maximum value of the sum of the drifts of the three frames at each storey for all the storeys $(\sum \delta_y)$max, and the overall sum for all the storeys of the sum of the drifts of the three frames at each storey $\sum(\sum \delta_y)$.

With regards to the dampers, the values calculated were the total sum of the maximum damper forces for the dampers in only the y-direction ($\sum F_{Djy}$) and for those in both directions ($\sum F_{Dj}$). Figs. 11 and 12 show the comparison between the different distributions of the summary parameters defined for each response quantity. For the sake of brevity, these figures refer to the cases where the supplemental damping ratio is 20% and to the first two summary parameters. Fig. 13 illustrates the results regarding the maximum damper forces.

In addition to these figures, a table is included for each supplemental damping ratio, where the percentage difference between the value obtained for each distribution of damping coefficients relative to the SEESPD distribution applied using the extended method was evaluated for each summary parameter (Tables 6 and 7).

The ranges of variations of the summary results relative to the peak and residual drifts are discussed in the following. Assuming ξ_{ve1}=10%, the maximum reduction given by the other distributions when compared with the SEESPD applied with the extended method, was equal to -6%, except for the parameter ($\sum\delta y$)*max*, where the SEESPD applied using the simplified method gave a reduction of -12% (Table 6). By assuming, instead, ξ_{ve1} =20%, the maximum reduction was -15%, except for the parameter ($\sum\delta y$)*max*, where the SEESPD applied using the simplified method gave a reduction of -21%. On the other hand, the maximum increase when compared with the SEESPD with the extended method was 9% for ξ_{ve1}=10% and up to 17% if ξ_{ve1} =20% (Table 7). Examining the peak floor accelerations, similar reductions were observed for ξ_{ve1}=10% or 20% and considering both the simplified and extended methods (Tables 6 and 7).

The maximum reduction when compared with the SEESPD obtained with the extended method was -15%. In addition, the UD and MPD also gave good results in terms of peak floor acceleration.

The previously mentioned ranges of variation in the summary results of the examined response parameters can be considered as not particularly significant, taking into account that many of them are limited to only a few percentage points, that the maximum reduction in a peak response quantity when compared with the SEESPD applied using the extended method is 14%, and above all that these variations and reductions are relative to response quantities already significantly reduced when compared with the case of the bare frame (see Figs. 11-12) and are well within the acceptable ranges.

Considering the passage from the extended to the simplified method, there are variations in the examined response parameters and also reductions for the peak drifts, but the same observations made above are valid also in the case of these reductions. The reductions that emerge when passing from the extended to the simplified method were slightly larger for the SEESPD than for the other distributions (as previously observed). Referring to the peak drift, a reduction means that the drifts derived using the extended method were slightly larger than those obtained with the simplified method. This slight increase in drift is due to several reasons, such as the decrease of the damping ratio, which could be obtained by passing from calculating Eq. (6) using the larger damping coefficients obtained through the simplified method to the same calculation elaborated with the damping coefficients obtained with the extended method. The results obtained for the sum of the maximum storey values $\sum(\delta\_MAX)$ reflects the situation at all other storeys where the drifts were less than the maximum ones. In particular, lower reductions are observed when going from the extended to the simplified method than for the peak values, especially for the SEESPD.

With regards to the maximum damper forces, there are marked differences between the distributions under examination.

This is a consequence of the differences observed for the damping coefficients, already presented in detail in the previous Tables 3 to 5. In order to carry out a better evaluation, the summary values of the damping coefficients are also shown in Tables 6 and 7, together with those of the maximum damper forces. Except the IDPD, the other non-energy distributions did not provide large reductions in the total damper force when compared to the UD. The energy distributions, on the contrary, provided significant benefits in terms of total damper forces. On this point, the SEESPD provided the best results for both the damping coefficients and the maximum damper forces, considering only the dampers arranged in the *y*-direction or in both the principal directions. By comparing the SEESPD with the uniform distribution, a reduction of up to 60% was observed (taking the SEESPD as reference) for the total damping coefficients in the *y*-direction and up to 41% for the total damper force in the same direction when the extended method is applied, and a larger reduction in comparison with the UD applied with the simplified method. As a consequence of what was observed for the damping coefficients, the extended method provided a significant general improvement, in terms of reducing the damper forces for all the distributions, with the largest benefits found for the IDPD and the energy distributions (reductions from 20% to 25% of the total damper force).

The following two tendencies (Landi *et al.* 2015) are observed also here for the 3D asymmetric-plan cases examined. The first is a general reduction, from ξ_{ve1}=10% to ξ_{ve1}=20%, in the differences in the damper forces between all the distributions and the SEESPD (see Tables 6 and 7). The second tendency is a reduction in the differences when going from the damping coefficients to the maximum damper forces (in the *y*-direction). This result could be correlated to the efficiency of the different distributions, in terms of consistency between the distribution of the damping coefficients along the height and the distribution of the damper forces (Hwang *et al.* 2013). In detail, with uniform distribution, the damping coefficients are constant along the height, while the damper forces obtained with NLDA tend to decrease at the upper storeys. At these storeys, therefore, the dampers do not work efficiently to dissipate the energy. For the other distribution methods, the distribution of forces is more consistent with the distribution of the damping coefficients, and the best consistency was obtained, in almost all cases, with the energy methods.

Considering the modified SEESPD distributions applied with a supplemental damping ratio of 20% together with the extended method, the distribution denoted as SEESPD(2T) provided good results compared to the SEESPD. This is due to a modest increase in total costs, of 2% considering $\sum CNj$ and $\sum FDj$, together with a reduction in the structural response parameters of up to 5-8%, due to the protection of the frame on the stiffer side (ADG).

On the contrary, the SEESPD(4T) distributions involved a greater increase in total costs (8%) than the previous distribution, with about the same benefit in terms of structural performance.

5. Conclusions

Different in-plan and vertical distributions of the damping coefficients were investigated concerning the retrofit of a RC three-dimensional asymmetric-plan building with six floors and variable sized columns, considering a nonlinear behaviour for both the structures and the fluid-viscous dampers and two levels of supplemental damping. Two design criteria were considered for the dampers, with the in-plan asymmetry being neglected in the first case (simplified method) and included in the second (extended method).

In the design phase, the energy methods SEPD and SEESPD provided the greatest benefits in terms of the total sum of the damping coefficients. Compared to the simple method, the extended method produced a reduction in the total damping coefficient for almost all the distributions, which was more significant for the IDPD and the energy methods.

With the different distributions, the ranges of variations of the summary results of the examined response parameters can be considered not particularly significant, taking account that many of them are limited to few percentage points, that these variations are relative to response quantities already significantly reduced compared to the bare frame and well within acceptable ranges. It should be noticed that the value of ξ_{ve1} for the different methods was the same.

Examining the maximum damper forces, except for the IDPD, the other non-energy distributions did not provide significant reductions in the total damper force when compared to the UD. The energy distributions, on the contrary, provided significant benefits in terms of total damper forces, especially the SEESPD. The extended method, in comparison with the simplified one, allowed to obtain a significant general improvement, in terms of reduction of damper forces, for all the distributions, with the largest benefits for the IDPD and the energy distributions. The proposed modified SEESPD distribution applied with the extended method, allowed to reduce the slight increase of drifts observed for the SEESPD with the extended method, with a very limited increase of the total damper force.

Therefore, in the examined typical case, the energy methods confirmed to be a good solution also for the design of nonlinear viscous dampers to be inserted in 3D asymmetric-plan buildings, where the SEESPD provided the best reduction of cost (damping coefficients and maximum damper forces). The consideration of the plan-asymmetry in the design with the different damping distributions allowed to obtain a reduction of cost together with similar structural performances, while maintaining the simplicity of application of the considered design approach.

References

Aguirre, J.J., Almazán, J.L. and Paul, C.J. (2012), "Optimal control of linear and nonlinear asymmetric structures by means of passive energy dampers", *Earthq. Eng. Struct. Dyn.*, **42**(3), 377-395. https://doi.org/10.1002/eqe.2211.

Altieri, D., Tubaldi, E., De Angelis, M., Patelli, E. and Dall'Asta, A. (2018), "Reliability-based optimal design of nonlinear viscous dampers for the seismic protection of structural systems", *Bull. Earthq. Eng.*, **16**(2), 963-982. https://doi.org/10.1007/s10518-017-0233-4.

Chopra, A.K. (2001), *Dynamics of Structures: Theory and Applications to Earthquake Engineering*, Prentice-Hall, Upper Saddle River, N.J, USA.

Christopoulos, C. and Filiatrault A. (2006), *Principles of Passive Supplemental Damping and Seismic Isolation,* IUSS Press, Pavia, Italy.

Constantinou, M.C., Song, T.T. and Dargush, G.F. (1998), "Passive energy dissipation systems for structural design and retrofit", MCEER Monograph No. 1, Multidisciplinary Center for Earthquake Engineering Research, State University of New York at Buffalo, N.Y., U.S.A.

CSI (2009), Analysis Reference Manual for SAP2000. ETABS, and SAFE, Berkeley, California, U.S.A.

Dargush, G.F. and Sant, R.S. (2005), "Evolutionary aseismic design and retrofit with passive energy dissipation", *Earthq. Eng. Struct. Dyn.*, **34**(13), 1601-1626.

Diotallevi, P.P., Landi, L. and Dellavalle. A. (2012), "A methodology for the direct assessment of the damping ratio of structures equipped with nonlinear viscous dampers", *J. Earthq. Eng.*, **16**(3), 350-373. https://doi.org/10.1080/13632469.2011.618521.

Eurocode 8 (2003), Design of Structures for Earthquake Resistance. Part 1: General Rules, Seismic Actions and Rules for Buildings, European Committee for Standardization; Brussels, Belgium.

FEMA 273 (1997), Guidelines for the Seismic Rehabilitation of Buildings, ATC for FEMA, Washington D.C., U.S.A.

FEMA 274 (1997), Commentary on the Guidelines for the Seismic Rehabilitation of Buildings, ATC for FEMA, Washington D.C., U.S.A.

FEMA 450 (2003), Recommended Provisions for Seismic Regulations for New Buildings and other Structures, BSSC for FEMA, Washington D.C., U.S.A.

Fujita, K., Kasagi, M., Lang, Z., Penfei, G. and Takewaki, I. (2014), "Optimal placement and design of nonlinear dampers for building structures in the frequency domain", *Earthq. Struct.*, **7**(6), 1025-1044. http://dx.doi.org/10.12989/eas.2014.7.6.1025.

Garcia, M., De La Llera, J.C. and Almazán, J.L. (2007), "Torsional balance of plan asymmetric structures with viscoelastic dampers", *Eng. Struct.*, **29**(6), 914-932. https://doi.org/10.1016/j.engstruct.2006.06.022.

Hahn, G.D. and Sathiavageeswaran, K.R. (1992), "Effect of added-damper distribution on the seismic response of buildings", *Comput. Struct.*, **43**(5), 941-950. https://doi.org/10.1016/0045-7949(92)90308-M.

Huang, X. (2018), "Evaluation of genetic algorithms for the optimum distribution of viscous dampers in steel frames under strong earthquakes", *Earthq. Struct.*, **14**(3), 215-227. https://doi.org/10.12989/eas.2018.14.3.000.

Hwang, J.S., Lin, W.C. and Wu, N.J. (2013), "Comparison of distribution methods for viscous damping coefficients to buildings”, *Struct. Infrastr. Eng.*, **9**(1), 28-41. https://doi.org/10.1080/15732479.2010.513713.

Istruzioni NTC (2009), Istruzioni Per L’applicazione Ddelle Norme Tecniche per le Costruzioni, (Italian Building Code Instructions), Italian Public Works Ministry, Rome, Italy.

Landi, L., Conti, F. and Diotallevi, P.P. (2015), “Effectiveness of different distributions of viscous damping coefficients for the seismic retrofit of regular and irregular RC frames”, *Eng. Struct.*, **100**(1), 79-93. https://doi.org/10.1016/j.engstruct.2015.05.031.

Landi, L., Diotallevi, P.P. and Castellari, G. (2013), “On the design of viscous dampers for the rehabilitation of plan-asymmetric buildings”, *J. Earthq. Eng.*, **17**(8), 1141-1161. https://doi.org/10.1080/13632469.2013.804893.

Landi, L., Lucchi, S. and Diotallevi, P.P. (2014), “A procedure for the direct determination of the required supplemental damping for the seismic retrofit with viscous dampers”, *Eng. Struct.*, **71**(15), 137-149. https://doi.org/10.1016/j.engstruct.2014.04.025.

Lavan, O. and Levy, R. (2010), “Performance based optimal seismic retrofitting of yielding plane frames using added viscous damping”, *Earthq. Struct.*, **1**(3), 307-326. https://doi.org/10.12989/eas.2010.1.3.307.

Lin, Y.Y. and Chang, K.C. (2003), “A study on damping reduction factor for buildings under earthquake ground motions”, *J. Struct. Eng.*, **129**(2), 206-214. https://doi.org/10.1061/(ASCE)0733-9445(2003)129:2(206).

Lopez Garcia, D. and Soong, T.T. (2002), “Efficiency of a simple approach to damper allocation in MDOF structures”, *J. Struct. Control*, **9**(1), 19-30. https://doi.org/10.1002/stc.3.

Lopez Garcia, D.A. (2001), “Simple method for the design of optimal damper configurations in MDOF structures”, *Earthq. Spectra*, **17**(3), 387-398. https://doi.org/10.1193%2F1.1586180.

Mazza, F. and Vulcano, A. (2011), “Control of the earthquake and wind dynamic response of steel-framed buildings by using additional braces and/or viscoelastic dampers”, *Earthq. Eng. Struct. Dyn.*, **40**(2), 155-174. https://doi.org/10.1002/eqe.1012.

Miyamoto, K., Taylor, D. and Duflot, F. (2002), “Seismic rehabilitation of a reinforced concrete hotel using fluid viscous dampers”, *Proceedings of the 12th European Conference on Earthquake Engineering*, London, U.K, March.

NISEE Software Library (1976), SIMQKE User Manual, University of California, Berkeley, U.S.A.

NTC (2008), Norme Tecniche per le Costruzioni (Italian Building Code), Italian Public Works Ministry, Rome, Italy.

Palermo, M., Muscio. S., Silvestri. S., Landi. L. and Trombetti. T. (2013), “On the dimensioning of viscous dampers for the mitigation of the earthquake-induced effects in moment-resisting frame structures”, *Bull. Earthq. Eng.*, **11**(6), 2429-2446. https://doi.org/10.1007/s10518-013-9474-z.

Panagiotakos, T.B. and Fardis, M.N. (2001), “Deformations of reinforced concrete members at yielding and ultimate”, *ACI Struct. J.*, **98**(2), 135-148.

Pollini, N., Lavan, O. and Amir, O. (2017), “Minimum-cost optimization of nonlinear fluid viscous dampers and their supporting members for seismic retrofitting”, *Earthq. Eng. Struct. Dyn.*, **46**(12), 1941-1961. https://doi.org/10.1002/eqe.2888.

Priestley, M.J.N., Calvi, G.M. and Kowalsky, M.J. (2007), *Displacement Based-Seismic Design of Structures*, IUSS Press, Pavia, Italy.

Ramirez, O.M., Constantinou, M.C., Gomez, J., Whittaker. A.S. and Chrysostomou, C.Z. (2002), “Evaluation of simplified methods of analysis of yielding structures with damping systems”, *Earthq. Spectra*, **18**(3), 501-530.

Ramirez, O.M., Constantinou, M.C., Kirche, C.A., Whittaker, A.S., Johnson, M.W., Gomez, J.D. and Chrysostomou, C.Z. (2000), “Development and evaluation of simplified procedures for analysis and design of buildings with passive energy dissipation systems”, Report No. MCEER-00-0010, State University of New York, Buffalo, U.S.\A.

SEISMOSOFT (2016), Earthquake Engineering Software Solutions, SeismoSignal Help System, SeismoSignal.

Silvestri, S., Gasparini, G. and Trombetti, T. (2011), “Seismic design of a precast r.c. structure equipped with viscous dampers”, *Earthq. Struct.*, **2**(3), 297-321. https://doi.org/10.12989/eas.2011.2.3.297.

Singh, M.P. and Moreschi, L.M. (2001), “Optimal seismic response control with dampers”, *Earthq. Eng. Struct. Dyn.*, **30**(4), 553-572. https://doi.org/10.1002/eqe.23.

Sorace, S. and Terenzi, G. (2008), “Seismic protection of frame structures by fluid viscous damped braces”, *ASCE J. Struct. Eng.*, **134**(1), 45-55. https://doi.org/10.1061/(ASCE)0733-9445(2008)134:1(45).

Sullivan, T.J. and Lago, A. (2012), “Towards a simplified Direct DBD procedure for the seismic design of moment resisting frames with viscous dampers”, *Eng. Struct.*, **35**, 140-148. https://doi.org/10.1016/j.engstruct.2011.11.010.

Symans, M.D. and Constantinou, M.C. (1998), “Passive fluid viscous damping systems for seismic energy dissipation”, *ISET J. Earthq. Technol.*, **35**(4), 185-206.

Takewaki, I. (1997), “Optimal damper placement for minimum transfer functions”, *Earthq. Eng. Sruct. Dyn.*, **26**(11), 1113-1124. https://doi.org/10.1002/(SICI)1096-9845(199711)26:11%3C1113::AID-EQE696%3E3.0.CO;2-X.

Takewaki, I., Yoshitomi, S., Uetani, K. and Tsuji. M. (1999), “Non-monotonic optimal damper placement via steepest direction search”, *Earthq. Eng. Struct. Dyn.*, **28**(6), 655-670. https://doi.org/10.1002/(SICI)1096-9845(199906)28:6%3C655::AID-EQE833%3E3.0.CO;2-T.

Tubaldi, E., Barbato, M. and Dall’Asta, A. (2015), “Efficient approach for the reliability-based design of linear damping devices for seismic protection of buildings”, *ASCE-ASME J. Risk Uncertain. Eng. Syst., Part A: Civil Eng.*, C4015009. https://doi.org/10.1061/AJRUA6.0000858.

Whittle, J.K., Williams, M.S., Karavasilis, T.L. and Blakeborough. A. (2013), “A comparison of viscous damper placement methods for improving seismic building design”, *J. Earthq. Eng.*, **16**(4), 540-560. https://doi.org/10.1080/13632469.2011.653864.

CC